Medical University – Varna
"Prof. Dr. Paraskev Stoyanov"

Department of General and Clinical Pathology, Forensic Medicine and Deontology

George Stoyanov Stoyanov, MD

Prognostic and predictive factors in *glioblastoma multiforme*

PhD summary

Advisor: Prof. Peter Ghenev, MD, PhD
Consultant: Assoc. Prof. Stoyan Pavlov, MD, PhD

Varna 2022

The dissertation is printed on 113 standard typewritten pages. It is supported by 65 figures, 13 tables and 250 literary sources, of which 11 in Cyrillic and 239 in Latin.

The official defense will take place on April 14, 2022 from …… .. hours in the second classroom of the Department of General and Clinical Pathology, Forensic Medicine and Deontology at the Medical University - Varna, at an open meeting of the Scientific Jury consisting of:

External members

Assoc. Prof. Margarita Kamenova, MD, PhD

Prof. Veselin Belovezhdov, MD, PhD

Prof. Nikolai Lazarov, MD, DSc

Spare external member

Assoc. Prof. Iliya Bivolarski, MD, PhD

Internal members

Assoc. Prof. Deyan Dzhenkov, MD, PhD

Prof. Anton Tonchev, MD, DSc

Spare Internal Member

Prof. Ara Kaprelyan, MD, DSc

Table of content:

1. List of commonly used abbreviations

- CBTRUS – central brain tumor registry of the United States
- cIMPACT-NOW - Consortium to Inform Molecular and Practical Approaches to CNS Tumor Taxonomy—Not Official WHO
- CK AE1/AE3 – cytokeratin cocktail
- CNS – central nervous system
- CT – computer tomography
- Diaph3 - Diaphanous Related Formin 3
- EGF-EGFR - epidermal growth factor - epidermal growth factor receptor
- GBM – *glioblastoma multiforme*
- GFAP – glial fibrillary acidic protein
- H3 – histone 3
- IDH – isocitrate dehydrogenase
- MGMT - O-6-methylguanine-DNA methyltransferase
- MRI – magnetic resonance imaging
- mTOR – mammalian target of rapamycin

- MLR – monocyte to lymphocyte ratio
- NLR – neurophil to lymphocyte ratio
- NEC – not elsewhere clasified
- NOS – not otherwise specified
- PLR – thrombocyte/platelet to lymphocyte ratio
- VEGF-VEGFR – vascular endothelial growth factor – vascular endothelial growth factor receptor
- WHO - World Health Organization

2. Introduction

Glioblastoma multiforme (GBM) is a malignant neoplasm of the central nervous system (CNS) (Louis *et al.*, 2021). GBM is one of the most malignant tumors in human pathology, in which, despite significant scientific and clinical studies over the past 50 years, patient survival has increased by an average of several months (Stoyanov and Dzhenkov, 2017).

GBM originates from precursors of astrocytic glia and/or mature glial cells and is classified as a primary tumor of the CNS - a representative of glial tumors, more commonly called gliomas (Altaner, 2008; McNeill, 2016). According to the current fifth edition of the World Health Organization (WHO) classification of CNS tumors from 2021, GBM is defined as:

"High-grade glioma with predominantly astrocytic differentiation, signs of nuclear atypia, cellular pleomorphism (in most cases), mitotic activity, diffuse growth, microvascular proliferation and/or necrosis that does not have a mutation in IDH" (Louis *et al.*, 2021).

Compared to the previous WHO classification of 2016 (revised fourth edition), some tumors that classically fit the description of GBM are now classified as diffuse astrocytoma with IDH mutation, WHO grade 4, and diffuse pediatric and pediatric type gliomas - hemispheric glioma (in the presence of the H3 G34 mutation), midline glioma (in the presence of

the H3 K27 mutation), and high-grade pediatric glioma (without mutations in H3 and IDH) (Louis *et al.*, 2021).

In terms of frequency, GBM is the most common primary tumor of the CNS, with an average incidence of 3-4 per 100,000 *capita*, and is characteristic of all ages, including congenital forms, but its highest incidence is after the fourth decade with an average age of diagnosis of 64 years (Ostrom *et al.*, 2017; Stoyanov *et al.*, 2018). Both genders are affected, with a slight predominance of males in terms of frequency (Ostrom *et al.*, 2017).

From a clinical point of view, GBM is a tumor with a fulminant course, which rarely gives neurological symptoms (hemiparesis, aphasia, visual disturbances, etc.), with the exception of cases of tumor localization in key CNS areas (Krex *et al.*, 2007). The most common symptoms are meningism, headache with migraine attacks, central vomiting, and epileptic seizures, which are the most common cause for patient presentations (Omuro and DeAngelis, 2013). Other, albeit less common, symptoms may be acute progressive behavioral disorders and cognitive changes (Hanif *et al.*, 2017; Omuro and DeAngelis, 2013). The fulminant development of the clinical picture leads to a rapid diagnosis, most often within six months after the initial onset of symptoms (IJzerman-Korevaar *et al.*, 2018; Ozawa *et al.*, 2018).

From a clinical point of view, the gold standard for diagnosing a CNS tumor is neuroimaging, such as ventriculography used in the past and more modern methods such as computed tomography (CT) and magnetic resonance

imaging (MRI) (Alper, 1999; Lutters and Koehler, 2018; Stummer *et al.*, 2006).

In imaging studies, GBM is described as a single, relatively large tumor formation with irregular borders and perifocal edema, in contrast to metastatic processes, which are most often multiple, rounded, and well-demarcated from the surrounding parenchyma (Cha *et al.*, 2007; p. Wang *et al.*, 2009). When performing contrast enhancement, the GMB contrasts on the periphery of the lesion, the so-called annular amplification, with central contrast absent due to the presence of extensive necrotic areas (Omuro and DeAngelis, 2013).

The formation may cover large areas of a particular lobe and even two lobes simultaneously (Agrawal, 2009; Dziurzynski *et al.*, 2012).

3. Aim and tasks

3.1 Aim

Based on the unresolved issues from the literature review, we aimed to study a cohort of patients with GBM, making a comprehensive analysis of age and gender characteristics, tumor size and location, the importance of the immune response, and survival and compare them with the MGMT profile of tumors and the significance of Diaph3 patterns of expression and intensity.

3.2. Tasks

To achieve this goal, we set ourselves the following tasks

1. Selection of tissue blocks from the archive of the Clinic of General and Clinical Pathology, University Hospital "St. Marina"- Varna, Varna, Bulgaria, for GBM cases diagnosed in the period February 2018 - February 2021
2. Reclassification of tumors according to the WHO classification from 2021 in order to unify the cohort according to the latest diagnostic requirements
3. Derivation of demographic characteristics of the cohort
4. Analysis of preoperative blood count for the number of neutrophils, platelets, monocytes, and lymphocytes
5. Establishment of the MGMT profile of the tumors
6. Establishing the image-diagnostic characteristics of tumors - tumor size and location

7. Preparation of three-dimensional reconstructions of the selected tumors with subsequent volumetric analysis
8. Study of the expression of Diaph3 in the cohort, as well as in an equal-sized control group of CNS material in autopsy cases without involvement of the nervous system from a pathological process and those with reactive gliosis
9. Study of the intensity of expression in rhythmic (Scherer) structures of growth
10. Statistical analysis and correlation of the obtained data

4. Materials and methods

For the established goals, we used:

4.1 Materials

1. Tissue sections from histologically proven GBM and an equal in size control group of non-tumor processes, n = 62 cases main group and n = 62 cases control group (of which n = 57 with normal brain parenchyma and n = 5 with reactive gliosis)

1.1 Excluding criteria - patients with histologically proven GBM and a second tumor in another location

1.2 Excluding criteria - patients with previously diagnosed GBM reoperated within the specified time interval

2. Data from the medical records concerning gender, age, preoperative blood count and postoperative survival

3. Neuroimaging data

4.2 Methods

1. Reclassification, according to the WHO classification for tumors of the nervous system, by:

1.1. Analysis of all histological sections and stains performed for the primary diagnosis

1.2. Immunohistochemical labeling with monoclonal mouse IDH1 R132H antibody (Sigma-Aldrich Prestige Antibodies, catalog number SAB4200548)

2. Export ratio of neutrophils to lymphocytes, platelets to lymphocytes, and monocytes to lymphocytes, in order to determine the equilibrium of the immune response to tumor growth, according to the formulas:

NLR = neutrophil count (10 ^ 9) / lymphocyte count (10 ^ 9)

PLR = platelet count (10 ^ 9) / lymphocyte count (10 ^ 9)

MLR = monocyte count (10 ^ 9) / lymphocyte count (10 ^ 9)

3. Immunohistochemical labeling with polyclonal rabbit MGMT antibody (Sigma-Aldrich Prestige Antibodies, catalog number HPA069497)

4. Analysis of computer tomographic and MRI imaging modalities of the CNS, performed at the stage of primary diagnosis

3.1. Analysis of the location, size, and contact of the tumor with critical structures for the central nervous system

5. Development of three-dimensional reconstructions of appropriate computer tomographic and MRI imaging studies for volumetric analysis

6. Immunohistochemical labeling of selected tumor paraffin sections with polyclonal rabbit Diaph3 antibody (Sigma-Aldrich Prestige Antibodies, catalog number HPA032151)

7. Selection of an equal volume cohort of control paraffin blocks (biopsy and necropsy) of patients without pathological changes in the central nervous system and those with reactive changes (non-tumor) to establish tumor specificity of Diaph3

The systematic research was conducted after obtaining permission from the Commission on Ethics of Research at the Medical University - Varna "Prof. Dr. Paraskev Stoyanov", Varna, Bulgaria, 93 / 21.05.2020.

Funding for the study was received from the Science Fund at the Medical University - Varna "Prof. Dr. Paraskev Stoyanov", Varna, Bulgaria, with project number 19010.

The following protocol was used for immunohistochemical labeling of paraffin tissue sections with IDH1, MGMT, and Diaph3:

1. Validation of antibodies and achievement of working concentration

1.1. IDH1 validated on positive control by GBM with molecularly verified mutation, with antibody working concentration 1: 1000

1.2. MGMT validation of positive control of prostate and palatine tonsils with working antibody concentration 1: 700

1.3. Diaph3 validated on positive prostate control with an operating concentration of 1: 700

In addition to validating the positive control, the described antibodies were titrated until an optimal response to the antibody concentration was achieved, and negative controls were performed on tissues without protein expression and absolutely negative control on tissues with and without protein expression, excluding the antibody from the protocol.

Digitization and automatic processing of the prepared slides

Selected primary biopsy specimens and immunohistochemical sections were digitized using an automated Leica Aperio Scanscope AT2 whole slide scanner (Aperio Technologies, Vista, CA). All sections were scanned at a magnification of x400, which allows for interactive full-section navigation with varying magnifications and detailed analysis using ImageScope V12.1.0.5029 software (Aperio Technologies, Vista, CA).

Cell counting was performed using the pre-programmed automated immunohistochemical expression analyzer QuPath. For our analysis, we used the precalibrated settings to use an already validated algorithm (Bankhead et al., 2017).

The statistical analysis was performed using the software package MaxStat Pro v3.6.

5. Results

5.1 Cohort

Accounting for the inclusion and exclusion criteria set for the cohort, it included a total of 62 cases (mean age 63.69 years, range 23-86 years), of which 33 male (mean age 59.85 years, range 23-85 years) and 29 female (mean age 68.07 years, range 52-86 years). Based on these characteristics, the male: female ratio in the primary cohort is 1.14: 1.

Based on the available paraffin blocks in the archive of the Clinic, 58 cases were selected from the primary cohort. The four cases initially removed from the cohort were due to the lack of paraffin tissue blocks explicitly requested by the patient and/or his relatives or the presence of a second tumor site in one patient - synchronous glioblastoma and non-small cell lung carcinoma. Of the remaining 58 cases, three more were eliminated in the second stage due to the minimal amount of tumor tissue in the paraffin blocks, which did not allow for scientific processing.

5.2 Reclassification of selected cases according to the criteria of the WHO classification for tumors of the nervous system from 2021

In order to define the diagnoses according to the new WHO requirements for CNS tumors from 2021, which require the evaluation of IDH R132H mutation, the cohort was unified according to this criterion. Although some patients had an initial biopsy answer of *glioblastoma multiforme*, NOS according to the 2016 classification, when performing IDH

R132H mutation status studies, some were excluded due to failure to meet the criteria for glioblastoma (n = 5) (Figure 5.1-2).

Compared to the demographic characteristics, according to the IDH R132H mutation, only young patients in the age group under 50 dropped out, with a higher share of IDH R132H mutation reported in females (n = 3).

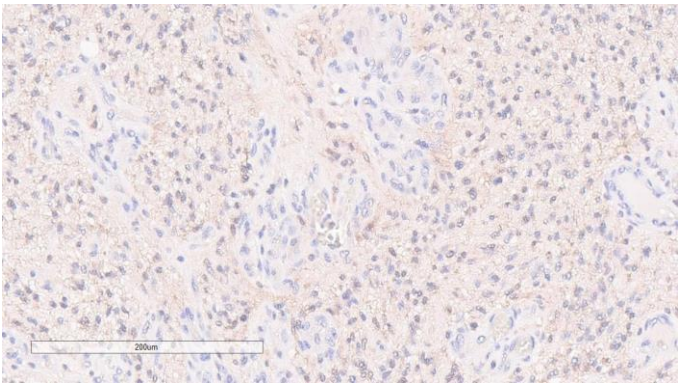

Figure 5.1 - IDH R132H mutant phenotype reclassified as Astrocytoma, WHO CNS grade 4 according to 2021 criteria, original magnification x200

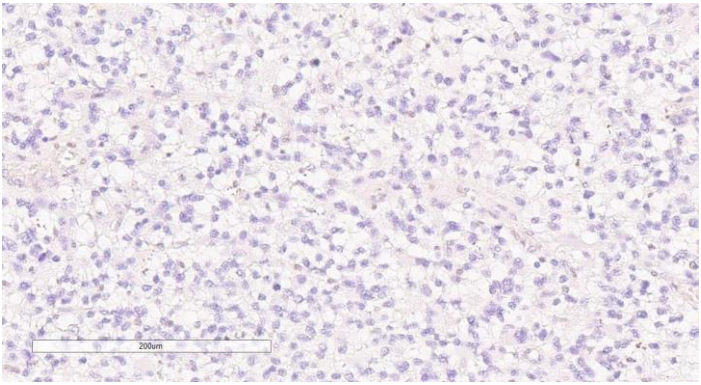

Figure 5.2 - Glioblastoma multiforme, without mutation in IDH, WHO CNS grade 4 according to the criteria of 2021, original magnification x200

5.3 Demographics

After reclassifying the tumors in the primary cohort, the cases designated as *glioblastoma multiforme*, without IDH mutation, WHO CNS degree of differentiation 4, were 50.

The demographic characteristics of our final cohort are as follows: 56% (n = 28) male, 44% (n = 22) female; male to female ratio 1.27:1; mean age 65.3 years, median 65 years, range 43-86 years (Figure 5.3-4).

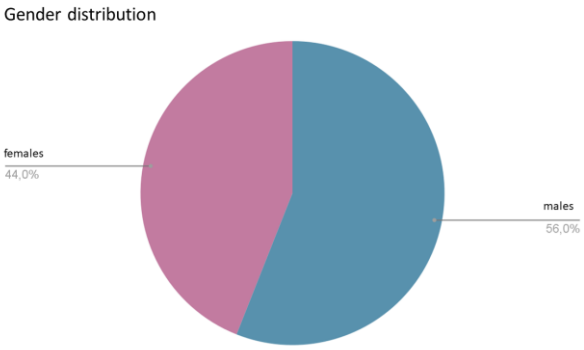

Figure 5.3 - gender distribution in glioblastoma multiforme

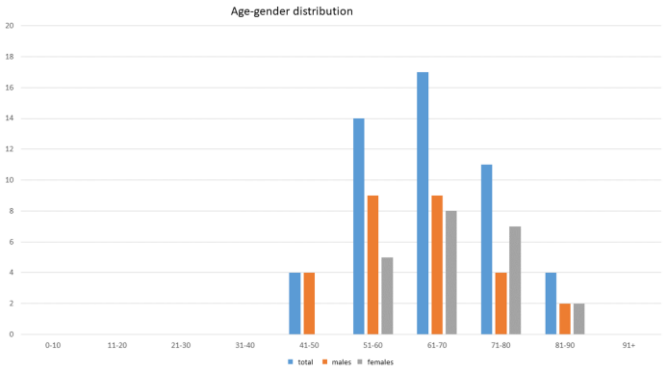

Figure 5.4 - Distribution of cases in the cohort by age groups

5.4 Frequency of MGMT promother methylation

Of the 50 cases in our cohort, 35% (n = 17) were positive for MGMT (Figure 5.5-6).

The mean age of patients with MGMT-positive GBM was comparable to that of the general cohort, with no statistically significant difference: mean age of 62.42 years (range 43-77 years) (Table 5.1). Gender distribution, in turn, shows that 42.84% (n = 8) of patients with MGMT-positive GBM are male, while 47.06% (n = 9) are female. These data show that although most patients with GBM are male (overall male: female ratio - 1.27:1), the incidence of MGMT mutation is higher in females (male: female ratio in MGMT positive tumors - 1: 1.3).

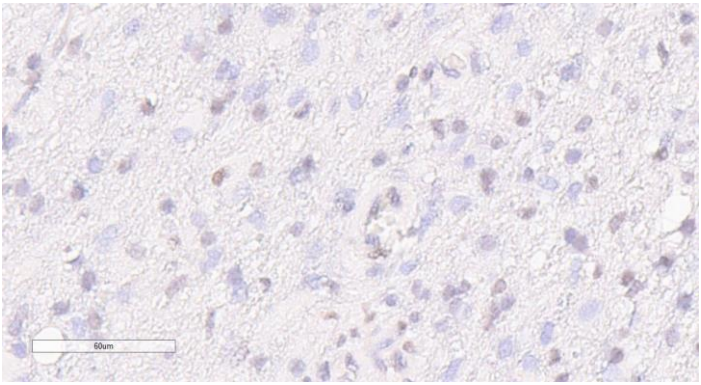

Figure 5.5 - glioblastoma multiforme, immunohistochemically positive for MGMT, original magnification x400

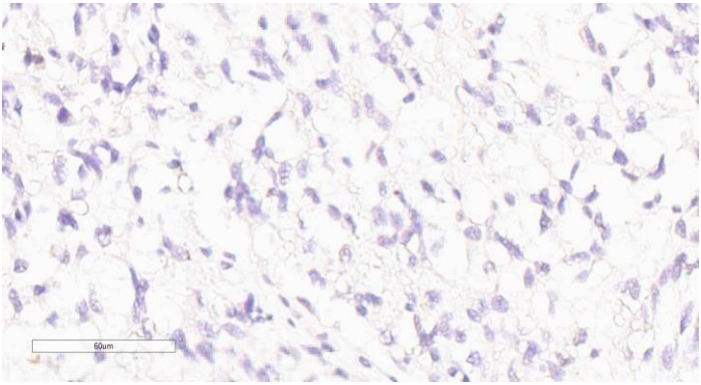

Figure 5.6 - glioblastoma multiforme, immunohistochemically negative for MGMT, original magnification x400

Table 5.1 - Age characteristics of the cohort and the MGMT profile of the tumors

value	total (n=50)	MGMT negative (n=33)	MGMT positive (n=17)
Mean age	65.3	66.79	62.42
median	65	66	62
mode	63	63 and 72	59
minimum	43	50	43
maximum	86	86	77

In men in the general cohort, the mean age of patients with MGMT-negative tumors was 64.65 years, and that in MGMT-positive was 58. In females in the general cohort, the

mean age of patients with MGMT-negative tumors was 70.08 years, and that of positive patients was 66.33 (Table 5.2).

Table 5.2 - age-gender characteristics of the cohort, according to the MGMT profile of the tumors

value	MGMT negative males (n=20)	MGMT positive males (n=8)	MGMT negative females (n=13)	MGMT positive females (n=9)
Mean age	64.65	58	70.08	66.33
Median	63	59	70	68
Mode	63 and 72	59	70	none
minimum	50	43	56	52
maximum	85	70	86	77

5.5 Tumor location and size

In the patients' medical records, data on the primary tumor location was present for 45 of the patients. In the remaining n = 5 patients of the cohort, the preoperative neuroradiological examinations were performed in an outpatient setting, and the operative interventions themselves were performed according to vital indications, not allowing for additional hospital-based neuroradiological examination preoperatively. In these patients, the medical records show only the laterality and localization of the process, and postoperative neuroradiological studies do not allow the interpretation of primary tumor size due to perifocal edema

and primary tumor localization due to the volume of resection involving more than one lobe.

In patients with hospital-based preoperative neuroradiological examinations (n = 45), 55.55% (n = 25) of the tumors were left-sided and the remaining 44.45% (n = 20) were right-sided (Figure 5.7).

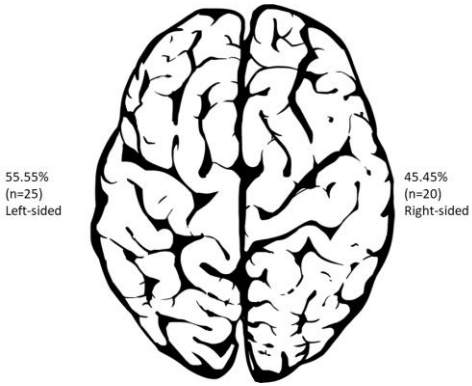

Figure 5.7 - Distribution of cases according to localization in the cerebral hemisphere.

In the cohort, a total of 40% (n = 18) of the tumors neuroradiologically involved more than one lobe of the cerebral hemispheres, with the lobe with the most extensive involvement being accepted as the primary localization. Of these tumors, 2.22% (n = 1) were true multicentric tumors involving both cerebral hemispheres but did not meet all the criteria for butterfly glioma. Compared to the location in the hemispheres, 24.44% (n = 11) cases were located in the frontal lobe, 37.78% (n = 17) in the temporal lobe, 28.89% (n = 13) in

the parietal lobe and 8.89% (n = 4) in the occipital lobe (Figure 5.8).

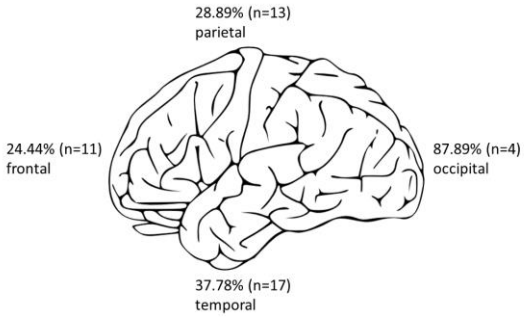

Figure 5.8 - Distribution of cases in the cohort according to localization in cerebral lobe

A complete topographic map of the tumor site in all cases shows that 13.33% (n = 6) of the cases are located on the left side of the frontal lobe and 11.11% (n = 5) on the right side; in the temporal lobe tumor, ones located on the left are 17.78% (n = 8) cases and right-sided ones are 20% (n = 9); in the parietal lobe left-sided tumors are 17.78% (n = 8) cases and right-sided ones are 11.11% (n = 5); in the occipital lobe, 6.67% (n = 3) of tumors were left-sided and 2.22% (n = 1) cases were right-sided (Figure 5.9).

The maximum tumor size in mm was derived from neuroradiological. From the obtained results and statistical analysis, it is evident that GBM at diagnosis has an average size of 50.51 mm (range 20-76 mm), with no statistically

significant difference in tumor size relative to the laterality of the process, except for parietal tumors (Table 5.3).

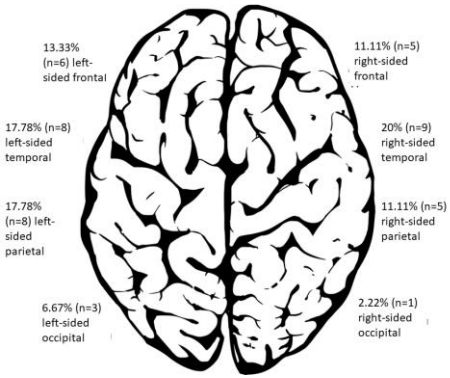

Figure 5.9 - distribution of cases in the cohort according to lobe localization and laterality

Table 5.3 - summarized descriptive characteristics of parietal lobe tumors

Value, in mm	total	Left sided	Right sided
Mean size	42.77	39.38	48.2
median	44	35.5	48
mode	48	none	none
minimum	21	21	31
maximum	76	76	60

In the current cohort, after detecting the tumor, there are no consecutive neuroradiological studies that allow for the analysis of tumor growth dynamics. Due to other indications, two of the patients had neuroradiological studies performed within a year before the diagnosis. The first patient, a 63-year-old male, underwent a brain CT scan due to suspicion of an acute cerebrovascular accident. On control CT and subsequent MRI eight months later, a tumor formation with a maximum size of 51 mm was found in the right frontal lobe (Figure 5.10). The second patient, a 74-year-old female, underwent a brain CT scan due to trauma, with only cortical atrophy of the brain parenchyma seen. Subsequently, the patient developed neurological symptoms, and 28 days later, on control CT and subsequent MRI occipitally on the right side, a tumor formation with a maximum size of 26 mm was seen (Figure 5.11).

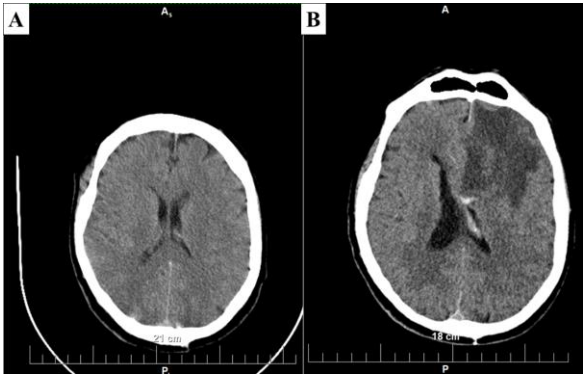

Figure 5.10 - CT of a 63-year-old patient: A - preserved structure of the brain parenchyma; B - large tumor formation

on the right frontal lobe, with unclear borders, eight months later

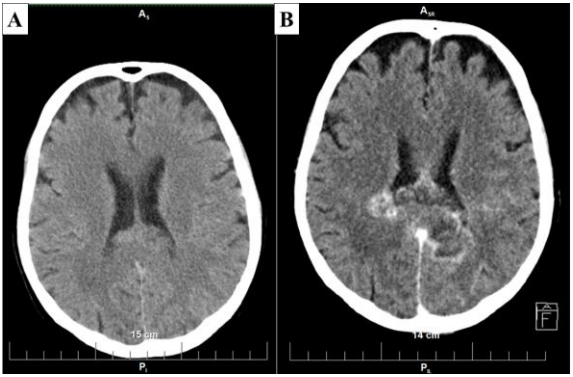

Figure 5.11 - CT of a 74-year-old female: A - cortical atrophy; B - tumor formation on the right occipital lobe with unclear borders and perifocal edema, 28 days later.

5.7 Survival

The average survival in the cohort (n = 50) from the day of surgery to the day of death was 255.96 days (8.41 months), and it is essential to note that five of the patients are still alive, i.e., the actual final survival is undoubtedly higher (Table 5.4). The survival range is from 18 days to 1061 days, with the longest overall survival being in a patient who is still alive 1150 days (37.78 months) after surgery. The survival rate on the first year is 26%, on the second - 8%, and given the short follow-up of the cohort, the survival on the third year is 4%. However, in this indicator, there is a significant difference according to the MGMT status of the tumors, as in MGMT

positive tumors, the survival of the first, second, and third years are 58.82%, 23.53%, and 11.76%, respectively.

Table 5.4 - survival in the cohort, in days and months

value	In days	In months
Mean survival	255.96	8.41
median	185	6.08
mode	none	none
minimun	18	0.59
maximum	1150	37.78

The average survival for males was 274.43 days (9.02 months) compared to 232.46 days (7.64 months) for females (Table 5.5).

Table 5.5 - survival of males and females in the cohort

value	males	females
Mean survival	274.43	232.46
median	239	112.5
mode	none	97 and 127
minimum	23	18
maximum	1150	1061

5.8 Systemic immune responce

Data from preoperative blood counts were present for only 22 patients in the cohort.

5.8.1 Neurthophil to lymphocyte ratio

As a limit value for the ratio of neutrophils to lymphocytes (NLR), we used NLR 4, an established index in many other malignancies. In the cohort, a total of eight patients had an NLR> 4, with the highest NLR index of 77.17. The remaining 14 patients had NLR <4 and the lowest NLR index of 1.81.

5.8.2 Thrombocyte to lymphocyte ratio

As a limit for the platelets to lymphocytes (PLR) ratio, we used PLR 200, a well-established index in many other malignancies. In the cohort, five patients had a PLR> 200, with the highest PLR index of 301.74. The remaining 17 patients had a PLR <200 and a lowest PLR index of 43.73.

5.8.3 Monocyte to lymphocyte ratio

As a limit value for the ratio of monocytes to lymphocytes (MLR), we used MLR>0.45. In the cohort, a total of five patients had an MLR > 0.45, with the highest MLR index of 4.07. The remaining 17 patients had an MLR <0.45 and a lowest MLR index of 0.09.

5.9 Diaph3 expression

5.9.1 Diaph3 expression in healthy brain parenchyma

At a concentration of 1: 700, in normal brain controls, antibody expression was cytoplasmic, mild to moderate in intensity, fine-grained, and present only in single cells of the cerebral cortex with neuronal and astroglial morphology. and cell positivity was not detected in the white matter (Figure 5.12-13).

Weak in intensity but uniform reaction - in the white and gray matter, was found in the endothelial cells of the vessels (Figure 5.14).

Uniform fine-grained and low-intensity expression in healthy controls was also seen in the meninges (Figure 5.15).

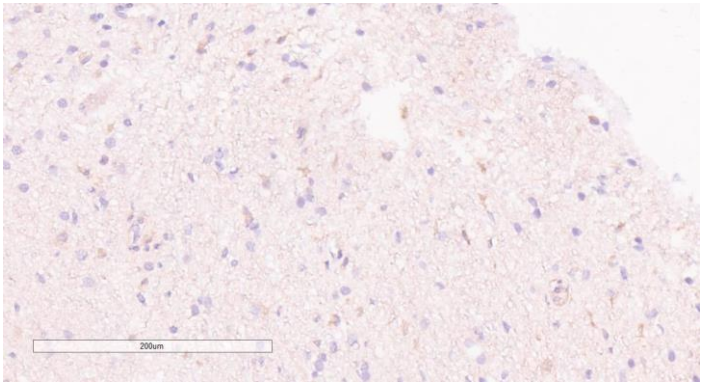

Figure 5.12 - Single weak to moderately intensely positive cells in the cerebral cortex of healthy controls, immunohistochemical labeling with Diaph3, original magnification x200

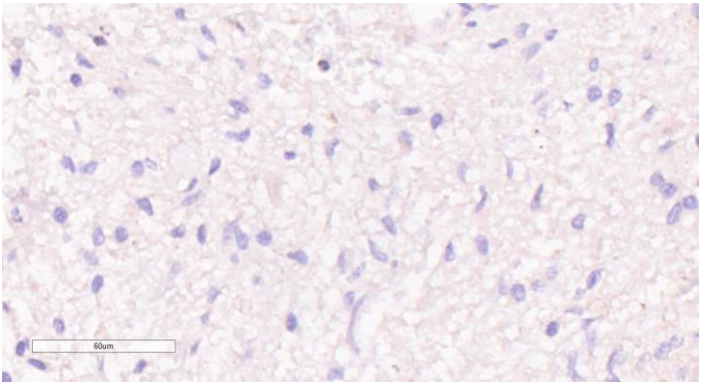

Figure 5.13 - Lack of cellular positivity in the white matter of healthy controls, immunohistochemical labeling with Diaph3, original magnification x400

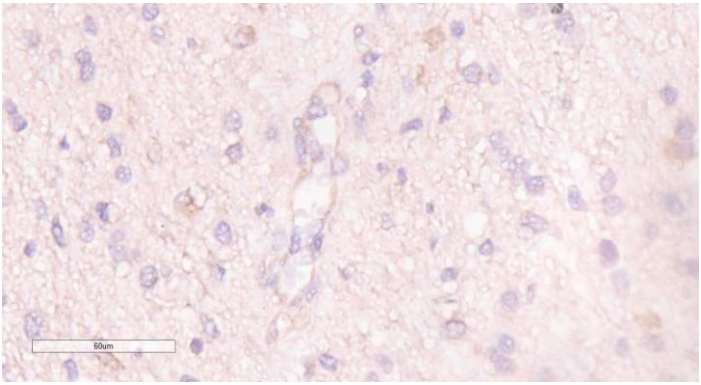

Figure 5.14 - Low to medium -intense reaction in the endothelial cells of a small vessel in the cerebral cortex, immunohistochemical labeling with Diaph3, original magnification x400

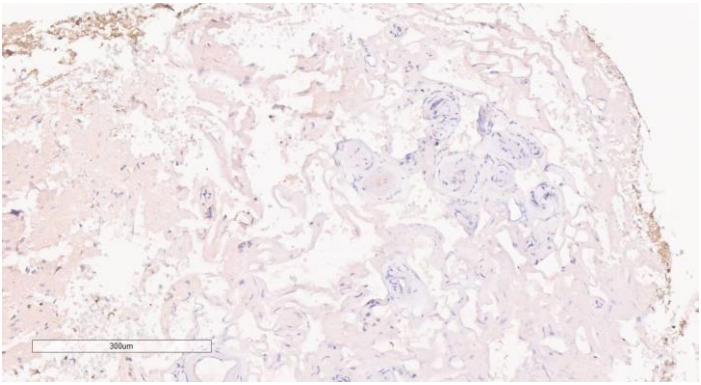

Figure 5.15 - Low-intensity expression in the meninges, immunohistochemical labeling with Diaph3, original magnification x100

5.9.2 Diaph3 expression in reactive gliosis

The control group also included five cases of reactive gliosis in different areas of the CNS due to a cerebrovascular accident, trauma, or a benign tumor compressing the brain parenchyma. In these controls, a more intense background staining was observed, as well as high-intensity fibrillar expression mainly in the cytoplasmic projections of cells with astrocytic morphology and nuclear expression in single cells with lymphocytic morphology located perivascularly (Figure 5.16). This form of expression in lymphocyte nuclei is of interest because it shows that Diaph3 is also involved in nuclear remodeling in the state of elevated transcription and/or mitosis.

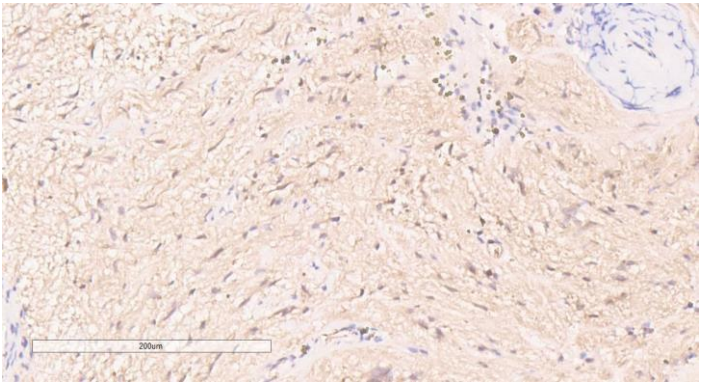

Figure 5.16 - Reactive gliosis in brain tissue peripheral to a benign vascular tumor, immunohistochemical labeling with Diaph3, original magnification x200

5.9.3 Diaph3 expression in *glioblastoma multiforme*

In our cohort (n = 50 - 100%), all tumors showed a positive reaction to the Diaph3 antibody at a concentration of 1: 700. The response was moderate to high-intensity, granular, and predominantly cytoplasmic; however single cells also showed a mild to moderate fibrillar nuclear reaction (Figure 5.17).

In terms of diffusion, the reaction was heterogeneous, with individual areas of the tumor parenchyma located centrally in the tumor formation itself, showing low intensity to no antibody expression (Figure 5.18).

Heterogeneity in terms of expression was also found in all types of Scherer figures, with the most intense expression seen in the areas of pseudopalisadic necrosis -

primary Scherer figures (Figure 5.19). In these sometimes extensive areas of the tumor parenchyma, high-intensity antibody expression was seen, as expected, given the proven phenomena of tumor migration outside the necrotic focus and the characteristics of Diaph3 as a molecule actively involved in cytoskeletal remodeling during cell movement.

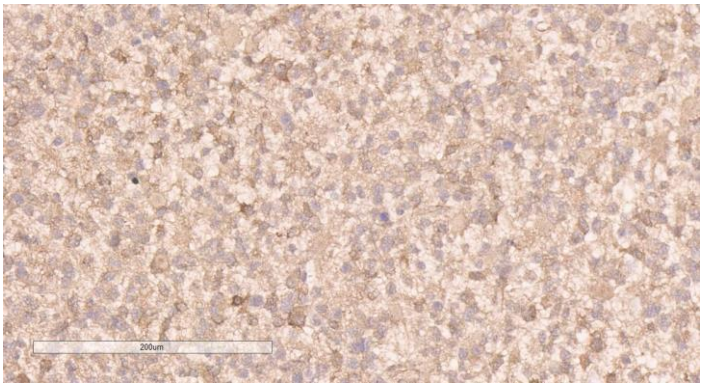

Figure 5.17 - High and moderately intense expression of Diaph3 in glioblastoma multiforme, original magnification x200

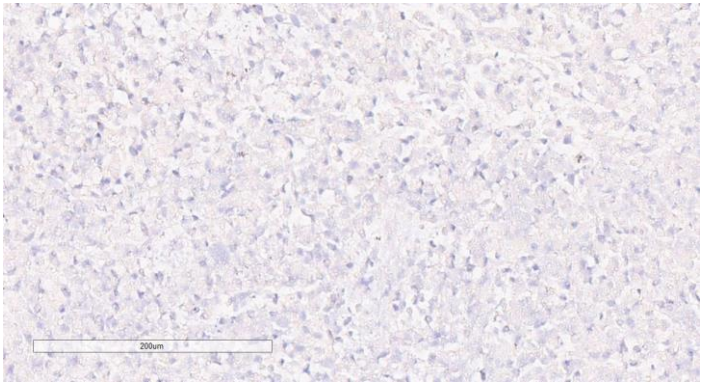

Figure 5.18 - Low intensity to no expression in the central parts of glioblastoma multiforme, immunohistochemical labeling with Diaph3, original magnification x200

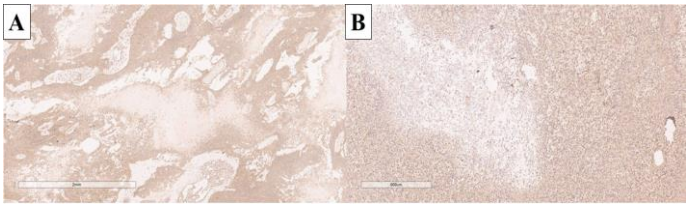

Figure 5.19 - High-intensity expression in cells around pseudopalisadic necrosis, immunohistochemical labeling with Diaph3: A - original magnification x20; B - original magnification x40

Among the secondary Scherer figures, the closest to expression in normal tissues was observed in the endothelial cells of glomeruloid vascular proliferations (Figure 5.20).

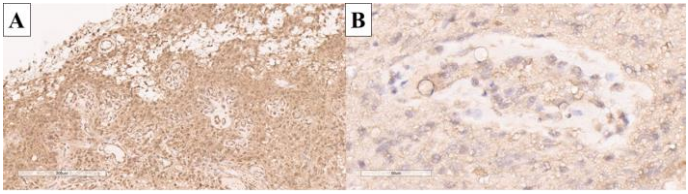

Figure 5.20 - Moderate to high-intensity antibody expression in endothelial cells of glomeruloid vascular proliferation, immunohistochemical labeling with Diaph3: A - original magnification x200; B - original magnification x400

In the borderline zone of transition from tumor parenchyma to grossly non-involved brain parenchyma

correlating to the neuroradiological phenomenon of perifocal edema, an expression gradient was observed (Figure 5.21).

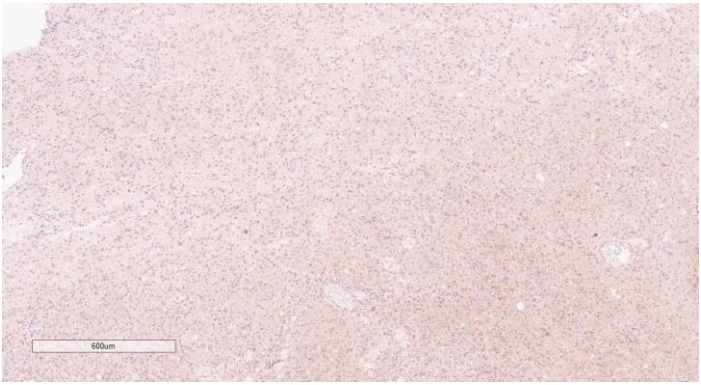

Figure 5.21 - Gradient in antibody expression from high to moderate intensity in hypercellular areas, to low intensity in normocellular areas, immunohistochemical labeling with Diaph3, original magnification x40

High to moderately intense expression in single cells, correlating with Scherer's secondary figures, were reported in these gradient zones. From Scherer's secondary figures, expression measurement was not possible only in the case of the phenomenon of neuronal satellitosis, given the presence of Diaph3-positive neurons in healthy brain controls.

Moderate to high-intensity expression in single cells in the marginal zone was reported in areas of vascular satellitosis, where expression in migrating tumor cells is higher in intensity than the expression seen in small vessel endothelial cells (Figure 5.22).

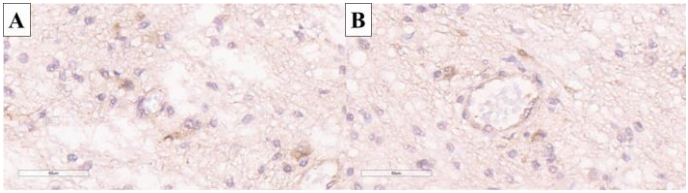

Figure 5.22 - Increased number of positive cells with moderate to high-intensity expression in the brain parenchyma, seemingly uninvolved by the tumor process, located around the small vessels, immunohistochemical labeling with Diaph3; A and B - original magnification x400

Tractal aggregation had an identical characteristic of antibody immunoexpression (Figure 5.23), where a parallel arrangement of longitudinally located small cells with moderate to high-intensity immunoreactivity was observed.

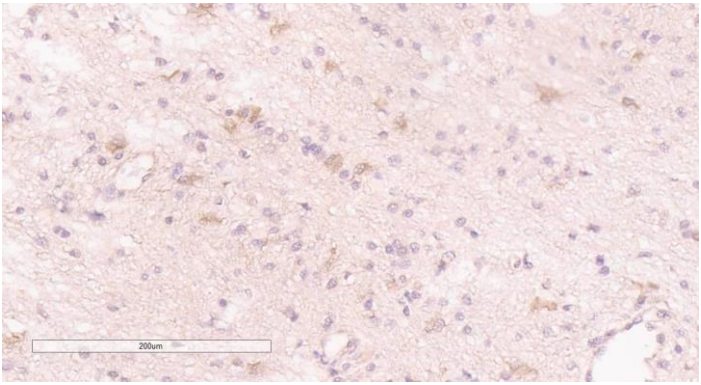

Figure 5.23 - longitudinal and parallel arrangement of groups of cells with moderate to high-intensity reaction in a seemingly normocellular, grossly non-involved area,

immunohistochemical labeling with Diaph3; original magnification x200

Significant gradients in antibody expression were observed in cases where the tumor grossly and histologically involved the cerebral cortex to its border with the meninges (Figure 5.24). Of particular interest here is that the described gradient is towards complete loss of immunoexpression in the areas of the submeningeal palisade (Figure 5.25).

Beyond the diagnostic criteria and growth phenomena, strong immunoreactivity for the antibody was observed in angiocentric macro-rosettes around large blood vessels without invasion in them (Figure 5.26). This phenomenon is most likely closely related to vascular satellites, with tumor cells first engaging large vessels and then spreading to their small branches.

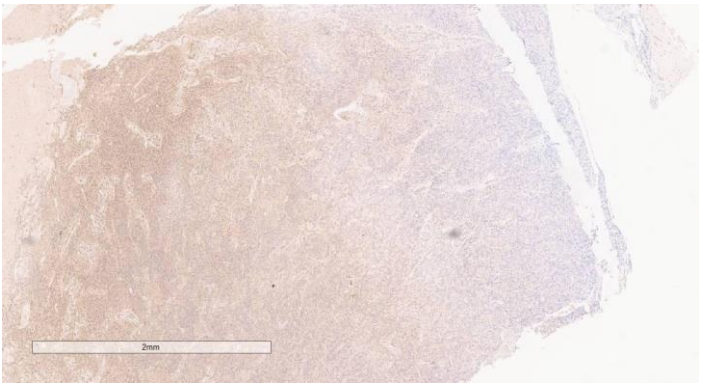

Figure 5.24 - gradient in the immunoexpression of glioblastoma multiforme involving the entire thickness of the

cerebral cortex, immunohistochemical labeling with Diaph3, original magnification x20

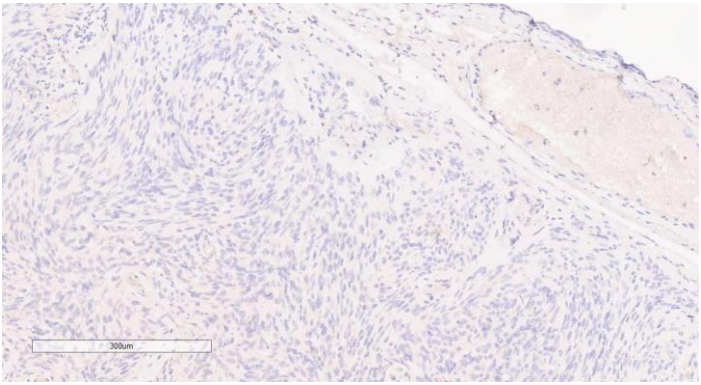

Figure 5.25 - loss of immunoreactivity of glioblastoma multiforme cells in the area of a submeningeal palisade, immunohistochemical labeling with Diaph3, original magnification x100

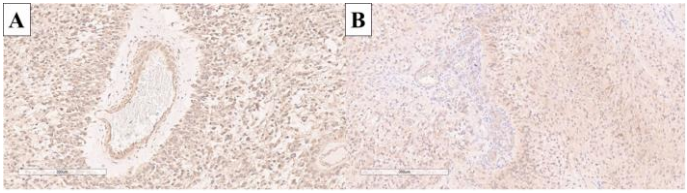

Figure 5.26 - macro-rosettes around large-caliber blood vessels - tumor cells have high-intensity immunoreactivity but do not penetrate the vessel wall, immunohistochemical marking with Diaph3: A - a cross-section of a large vessel, original magnification x100; B - longitudinal section of a vessel of medium caliber, original magnification x100

Against the background of this substantial heterogeneity of Diaph3 expression in different areas of the tumor, using the algorithm for automated counting of positive cells in the tumor indicated in the chapter Material and methods, substantial variability in the ratio of positive cells in the tumor parenchyma was observed, with a mean percentage of expressing tumor cells in the parenchyma of 62.66%, range 12-96% (Table 5.12).

Table 5.6 Descriptive characteristics of Diaph3 expression in glioblastoma multiforme

value	*Diaph3 (%)*
mean	62.66
median	61.5
mode	53 and 90
minumum	12
maximum	96

5.10 Statistical analysis

As already mentioned, the average survival of patients in the cohort is 255.96 days (8.41 months), which is higher in males - 274.43 (9.02 months) compared to 232.46 days (7.64 months) in females, and this difference is not is statistically significant p> 0.05 (Figure 5.27).

Regarding the laterality of the process - left-sided versus right-sided, the average survival in left-sided tumors is 254.41 days, compared to 257.78 in right-sided tumors, and the difference in survival is again not statistically significant - p> 0.05 (Figure 5.28).

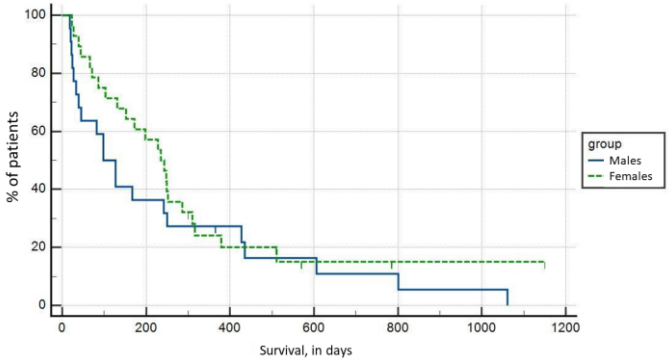

Figure 5.27 - Kaplan-Meier survival analysis by gender

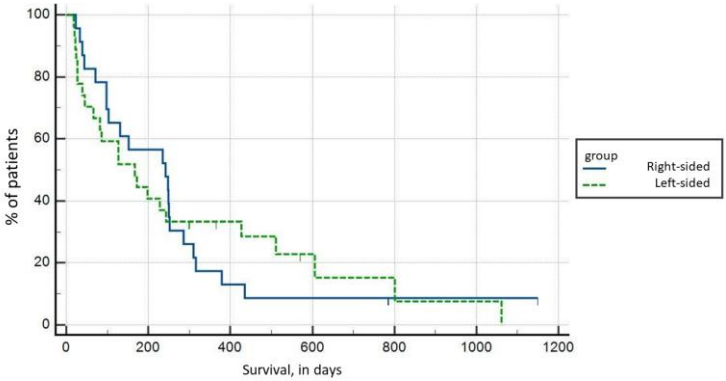

Figure 5.28 - Kaplan-Meier survival analysis on laterality of the tumor

Regarding the tumor size, the tumors were divided into 6 groups, and the average survival in them was as follows: 20-30 mm - 237.4 days; 31-40mm - 500.8 days; 41-50mm - 193.67 days; 51-60mm - 169.36 days; 61-70mm - 248.5 days and 71 + mm - 585.25 days. In terms of tumor size, the groups were extremely diverse, both in survival and the number of cases, ranging from four cases in the 71 + mm group to 12 cases in the 41-50 mm group. Comparison of survival by groups using the 1-way ANOVA test and Kaplan-Meier survival analysis showed no statistically significant difference in the survival of the different groups, p> 0.05 (Figure 5.29).

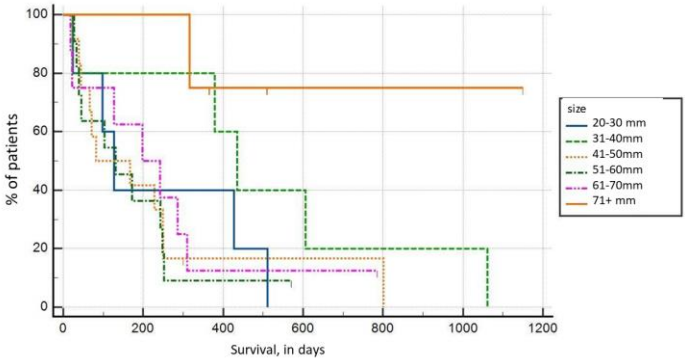

Figure 5.29 - Kaplan-Meier survival analysis relative to primary tumor size

The most significant difference in survival was found based on MGMT status, where the mean survival of patients in the cohort of MGMT-positive tumors was 477.77 days (15.7 months) versus 141.58 days (4.65 months) with a statistical significance of p <0.0001 (Figure 5.30).

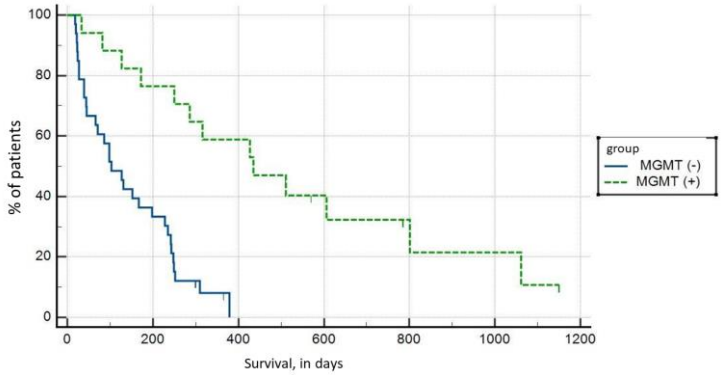

Figure 5.30 - Kaplan-Meier survival relative to MGMT status

Compared to tumor localization in lobes, in frontal tumors, the average survival is 248 days, in temporal - 284.94 days, in parietal - 310.23 days, and occipital - 190.25 days. Again, significant differences in groups were observed in the number of cases in the group and the survival observed. 1-way ANOVA test and Kaplan-Meier analysis of survival did not show a statistically significant difference in survival, $p > 0.05$ (Figure 5.31).

Comparing the age groups, in the group 41-50 years, the average survival is 584.75 days, in the group 51-50 it is 306.43 days, in the group 61-70 it is 284.47 days, in the group 71-80 it is 104 days, and in the group 81-90 years, the mean survival is 47.25 days (Figure 5.36). The 1-way ANOVA test and Kaplan-Meier analysis showed a statistically significant difference in survival with $p = 0.0059$ (Figure 5.32). In the second stage, a post comparison Tukey test was performed, which found that the age group 41-50 years lived statistically

longer than the groups 71-80 and 81-90 years, and no statistically significant difference was found between the other groups (Table 5.17).

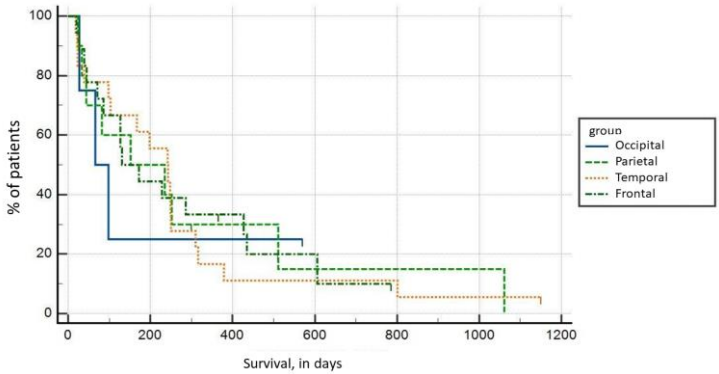

Figure 5.31 - Kaplan-Meier survival analysis relative to location in lobe

Table 5.7 - post comparison Tukey test to compare survival between different groups

41-50 survival compared to	Difference in survival	df	Statoistical significance
51-60	278.32	2.97	no
61-70	300.28	3.27	no
71-80	480.75	4.98	yes
81-90	537.5	4.6	yes

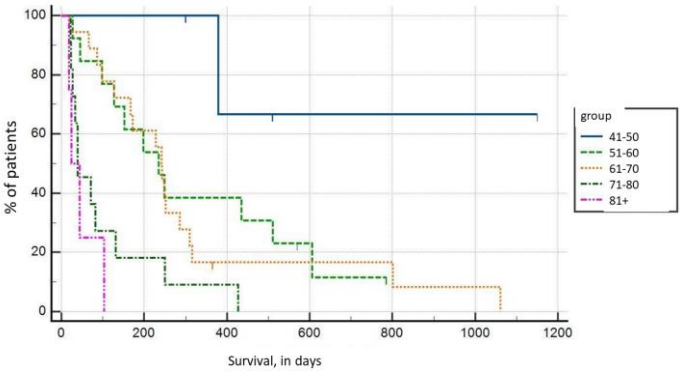

Figure 5.32 - Kaplan-Meier survival analysis relative to age group

Regarding the immune system's response, no correlation was found with the survival in patients with NLR> 4, p> 0.05, with a survival rate of 182.25 days, compared with 297.79 days in patients with non-elevated NLR (Figure 5.33).

Again, with p> 0.05, there was no statistically significant difference in survival in patients with PLR> 200, with a median survival of 130.8 days, compared with 292.53 days in patients with no elevation of PLR (Figure 5.34).

A statistically significant difference in survival, with p = 0.0044, was found in patients with MLR> 0.45, and in these patients, the survival was significantly lower - 103.83 days versus 313.13 days in patients with no elevation in the index (Figure 5.35).

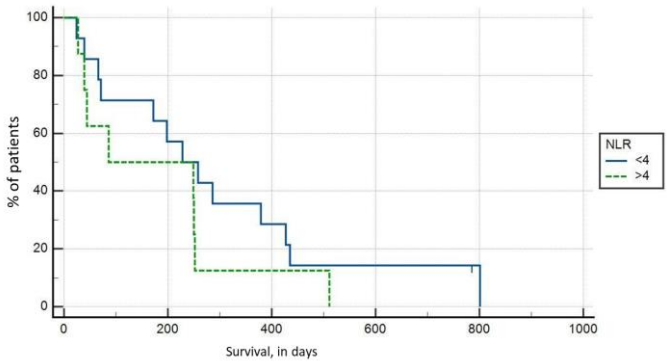

Figure 5.33 - Kaplan-Meier survival analysis of relative to NLR

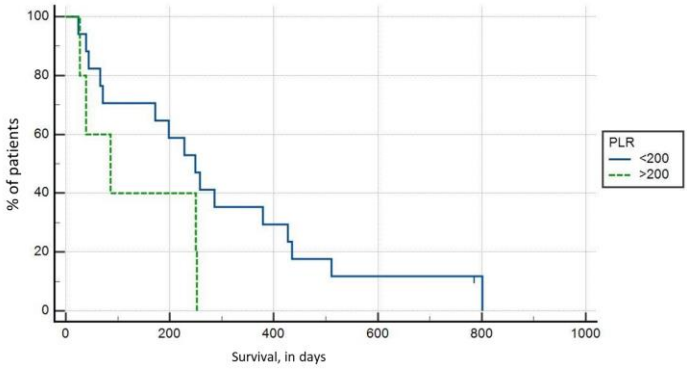

Figure 5.34 - Kaplan-Meier survival analysis relative to PLR

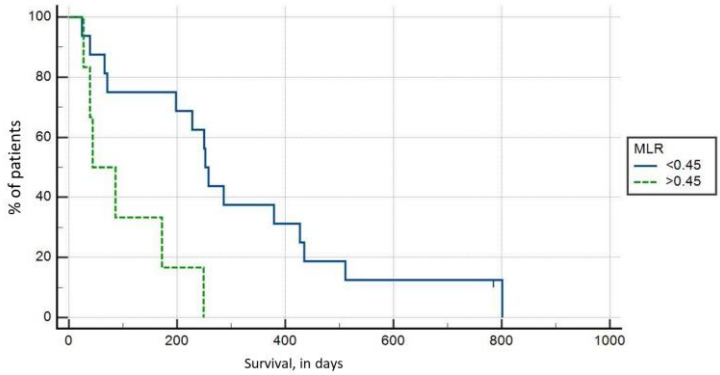

Figure 5.35 - Kaplan-Meier survival analysis relative to MLR

When calculating the combined index of elevated NLR and PLR; NLR and MLR; MLR and PLR; NLR, PLR, and MLR, it was found that statistically significant differences in survival were observed in patients with a combined increase in MLR and at least one more index. The established statistical values are as follows: patients with synergistically elevated NLR and PLR have no statistically significant difference in survival, p> 0.05, 130.8 versus 292.53 days; patients with synergistically elevated NLR and MLR had statistically significant lower survival, p = 0.0062, 100.25 versus 291.56 days; patients with synergistically elevated MLR and PLR had a statistically significant lower survival, p = 0.0044, 50.67 versus 288.16 days, and as all patients in this group had a synergistic increase in all three indicators - NLR, PLR, and MLR, again statistically significant lower survival was reported, p = 0.0044 (Figure 5.36-38).

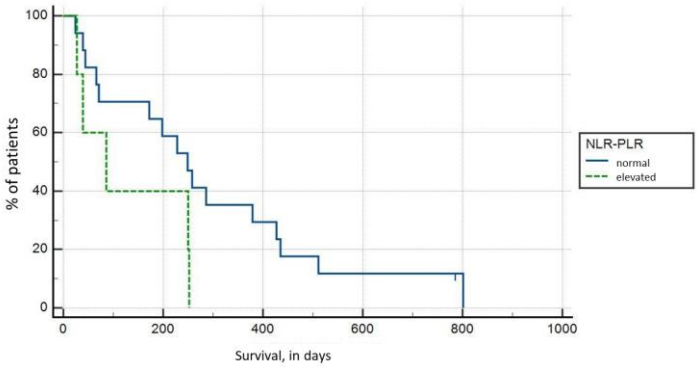

Figure 5.36 - Kaplan-Meier survival analysis relative to NLR and PLR

Regarding the percentage of Diaph3-expressing tumor cells, the cases in the cohort were divided dichotomously, with a cutoff value of 60% as the closest to the median round value. Thus, the two groups with a low and high expression included the closest number of tumors - n = 26 for those with high expression levels and n = 24 for those with low expression levels. Analysis of the significance of expression levels in patients' survival using the Kaplan-Meier method showed p> 0.05, with a mean life expectancy in the high expression group of 246.19 days versus 267.17 days (Figure 5.39).

Correlation analysis found no correlations between Diaph3 expression levels and age, gender, tumor location and size, p> 0.05 (Figure 5.40).

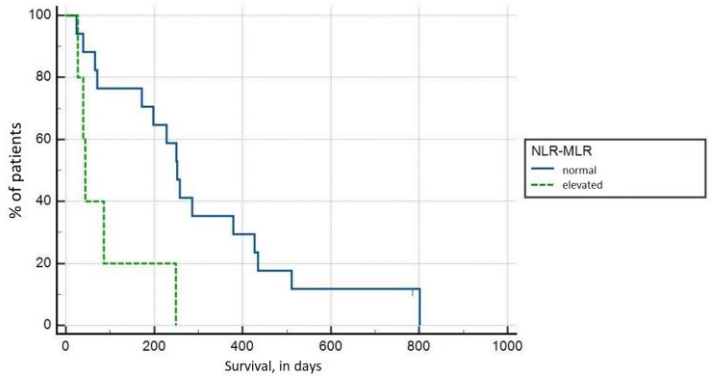

Figure 5.37 - Kaplan-Meier survival analysis relative to NLR and MLR

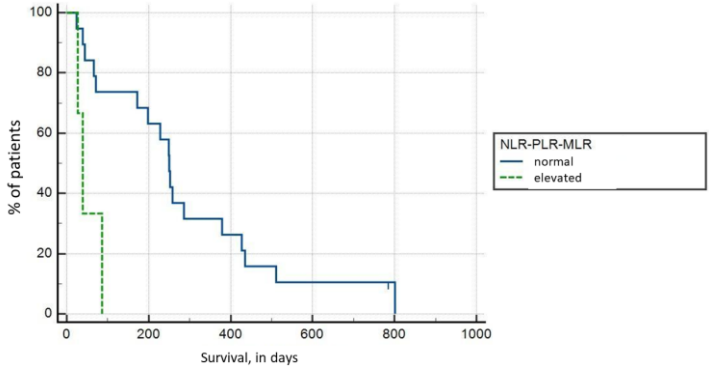

Figure 5.38 - Kaplan-Meier survival analysis relative to NLR, PLR and MLR

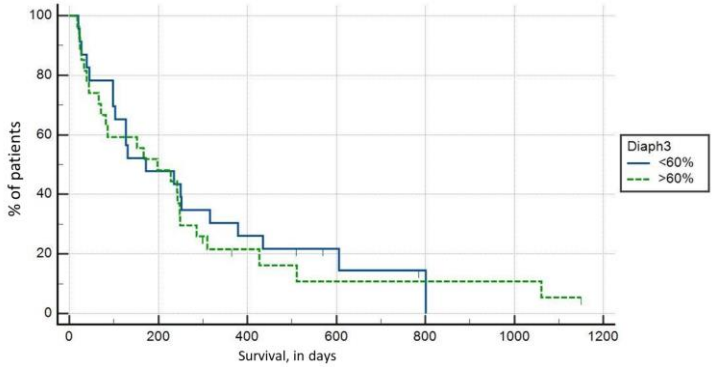

Figure 5.39 - Kaplan-Meier survival analysis relative to Diaph3 expression

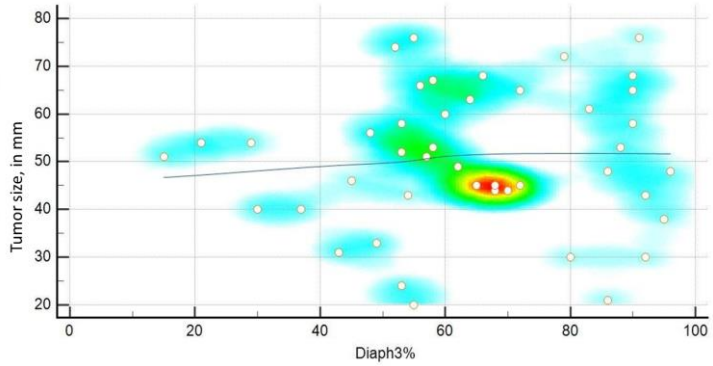

Figure 5.40 - Correlation analysis with heatmap to compare tumor size and Diaph3 expression

6. Discussiom

6.2 IDH R132H mutational status

In our cohort, as already mentioned, a mutant phenotype was found in 9.1% (n = 5) of a total of n = 55 patients in the primary cohort, allowing reclassification of tumors according to the new classification. These data are fully comparable to those of large cohorts, where the frequency of IDH R132H mutants, currently diffuse astrocytoma, WHO CNS grade 4, varies around 10% and other forms of mutation in IDH1, as well as mutations in IDH2, are extremely rare (Lai et al., 2011; Yan et al., 2009). The age-gender distribution is comparable to these data; mutant forms are more common in young people under the age of 50 and most common in females and the frontal lobe (Lai et al., 2011).

6.3 Frequency, demographics and survival

Given the cases reclassified in another group, the incidence of *glioblastoma multiforme* will not drastically change, which in our population, according to our data from a previous five-year cohort (n = 183), is 2.03 cases per 100,000 capita (Stoyanov et al., 2017), which is lower than the latest reported data from the United States - 3.23 cases per 100,000 capita, with a comparable median age of 65 years, with a significantly higher incidence in men - 4.04, compared to 2.53 per 100,000 capita for females (Ostrom et al., 2021).

However, a drastic difference will occur in the average age of onset of the disease, given that mutant forms are more

common in young people under 50 years of age, and there will also be a statistical increase in cases in men due to their higher incidence in females. For example, the current average age in the cohort is 65.3 years, while in our previous cohort, it was 59.18 (Dzhenkov, 2018). Another direct consequence of the change in classification is a reduction in the average survival of patients, given that longer surviving patients fall into another nosological unit. With these innovations in the classification, the changes can be summed up as - glioblastoma is a tumor characteristic of old age, more common in males, with poor prognosis.

For this reason, Kim defines *glioblastoma multiforme* from a clinical and epidemiological point of view and as a neurological disease characteristic of older men (Kim et al., 2021). On the other hand, Ostrom reports an average annual incidence of 3.99 per 100,000 capita for males and 2.52 per 100,000 capita for females, with similar age characteristics to our own and of our previous cohort (Ostrom et al., 2018; Stoyanov et al., 2017). Although based on the 2016 WHO classification, Ostrom also analyzed survival in parallel of GBM with and without IDH mutation in the same study. In the analysis of tumors without IDH mutation corresponding to *glioblastoma multiforme* according to the WHO classification for CNS tumors from 2021, the median established survival in the entire cohort of more than 200 individuals is 16.9 months, and the median survival in men is 15 months, and in females 25.5 months. Based on these epidemiological data and the derived survival in the cohort, GBM is a more common tumor in men and has a significantly worse prognosis in them.

As can be seen from the results in our cohort, there is no significant difference in survival between males and females, and the average survival rate for men is even higher than for females. The comparative analysis with CBTRUS shows that our cohort's average survival is significantly lower - 8.41 months against 16.9 months, i.e., more than twice as low (Ostrom et al., 2021). However, the survival in the current cohort is an encouraging indicator, given its significant increase compared to our previous cohort (n = 94), which in the presence of IDH mutant forms has an average survival of 197.5 days (6.49 months) (Dzhenkov, 2018). Despite the significantly lower average survival in our cohort, the survival of the first year - 26%, the second year - 8% and the third year 4% - is comparable to or close to those reported in other studies (Batash et al., 2017; Tamimi and Juweid, 2017; Thon et al., 2013; Witthayanuwat et al., 2018).

As can be seen from our sample and comparison with other cohorts, *glioblastoma multiforme* is a tumor with an abysmal prognosis. Despite the vast resources devoted to studying the biological behavior of tumors and the potential for pharmacological and nonpharmacological interventions, historical survival remains almost unchanged compared to other malignancies where there has been a significant reduction in mortality in recent decades, such as cervical carcinoma (Cervical Cancer - Cancer Stat Facts). As can be seen from the data of CBTRUS, our samples, limited data from the National Cancer Registry of the Republic of Bulgaria, and GLOBOCAN, GBM is the most common tumor of the nervous system and, according to some reports, has a higher incidence than some malignant diseases such as

laryngeal carcinoma, thyroid carcinoma and Hodgkin's disease with significantly higher public awareness (CBTRUS Fact Sheet 2021 - CBTRUS; Stoyanov et al., 2018, 2017; Sung et al., 2021; Werneck de Carvalho et al., 2017; Valerianova et al., 2017, 2015; Dzhenkov, 2018). Also, from the above large statistical samples, the higher frequency is evident, not only of GBM but also of all CNS tumors in developed countries, compared to developing ones (CBTRUS Fact Sheet 2021 - CBTRUS). This fact is, of course, mainly related to access to medical care and the existence of modalities for diagnosing these nosological units, rather than actual lower morbidity in these populations (Peters et al., 2008; Punchak et al., 2018; Weiss et al., 2020). Unfortunately, the lower morbidity found in our country compared to countries with high economic resources puts us in the group of countries with a relatively high rate of hidden morbidity (Ostrom et al., 2021; Stoyanov et al., 2018, 2017, 2017). Given the relatively high incidence of GBM in some regions, attempts at early diagnosis programs have been reported due to the impossibility of prevention, such as in malignant diseases of the cervix, lung, larynx, colon and stomach (Neugut et al., 2019). However, due to the lack of effective screening, unlike other malignancies such as prostate, colon, mammary and thyroid carcinomas, due to the need for equipment and staff for neuroradiological research, these programs are ineffective in the first place in terms of financial resources and benefit, due to lack of effect on the survival of early diagnosis (Croswell et al., 2010; Jakola et al., 2012; Komotar et al., 2008; Neugut et al., 2019; Verduin et al., 2018; Wang et al., 2014). Currently, the only cost-effective screening method, despite its low specificity, is the study of circulating levels of GFAP, which is more indicative of the

presence of a pathological process in the central nervous system and effective in monitoring these patients due to elevated circulating levels, due to elevated levels being present in all groups of tumors, including metastatic, in cerebrovascular, inflammatory and neurodegenerative diseases (Abdelhak et al., 2018; Jung et al., 2007; Puspitasari et al., 2019; Saraste et al., 2021; Sharquie et al., 2020; Tichy et al., 2015; Verberk et al., 2021).

6.4 MGMT mutational status

According to the WHO criteria for CNS tumors, a significant factor important for the survival of patients with *glioblastoma multiforme* is the MGMT mutation status, indicating the possibility of tumor response with temozolomide therapy. In our cohort, the incidence of MGMT-positive tumors was 35% (n = 17), which is comparable to the literature, where the incidence varies between 30% and 60% (Costa et al., 2010; Choi et al., 2021; Håvik et al. al., 2012; Incekara et al., 2020; Pandith et al., 2018). In our study, the difference in survival was statistically significant at p = 0.0001, with a mean survival in MGMT-positive tumors of 477.77 days versus 141.58 days in the negative ones, and the statistical significance was comparable to that reported by other authors as well as the mean duration of survival in positive cases (Annavarapu et al., 2021; Fuster-Garcia et al., 2021; Radke et al., 2019; Smrdel et al., 2016). A similar ratio is found in the first, second and third years (Izadpanahi et al., 2014; Ostrom et al., 2021). From these data, we can conclude that the significant difference in survival between ours and other similar studies is not due to MGMT

positive cases, where it is almost the same, but mainly due to MGMT negative cases, where survival is significantly below the reported (Izadpanahi et al., 2014; Ostrom et al., 2021).

6.5 Tumor location, size, growth and the role of neuroradiology

Concerning tumor localization, it is difficult in this transitional period of classification to compare with the literature data due to differences in the biological course of tumors with and without IDH mutation. One of the few analyzes of the localization of IDH mutant forms shows that they are most often seen in the frontal lobe (Lai et al., 2011). The IDH mutant form is a significant part of the group previously defined as secondary glioblastomas - arising from a previous low-grade glioma. These forms of GBM are by definition slow growing, less invasive, and smaller in size. However, they remain aggressive tumors, and in a general cohort. Stensjoen found that the daily rate of tumor volume increase was 1.4%, and the volume-doubling time was 49.6 days utilizing repeated neuroradiological studies in 106 patients prior to surgery. (Stensjøen et al., 2015). If we assume that 10% of the tumors in this sample lose their classification as GBM according to the WHO criteria from 2021, then the growth of the newly defined GBM is undoubtedly even more aggressive. In a smaller group (n = 32) with similar characteristics and methods, Wang found that the time to volume doubling was 17 days (Wang et al., 2009). In a case report of a 60-year-old male, Zhang illustrated the neuroradiological progression of *glioblastoma multiforme* from 7 mm to 13 mm on day 12, 17 mm on day 23 and

involvement of almost the entire hemisphere seven months after the first symptoms, suggesting *glioblastoma multiforme* doubles in size in about ten days (Zhang et al., 2016). As can be seen from the cases of our cohort, although only two patients have a previous hospital-based neuroradiological examination, *glioblastoma multiforme* is a tumor with fulminant development and rapid growth. Although based on only two neuroradiological studies, on the first of which no tumor is present, we cannot determine the tumor growth rate; however, the rapid growth is well underlined. This is best seen in the 74-year-old female patient, who developed a tumor with a maximum size of 26 mm in just four weeks.

Given the rapid growth of the tumor and its diffuse nature, which cannot be well established neuroradiologically, neurosurgical interventions in *glioblastoma multiforme* are not only tricky methodologically and with consequent neurological deficits but also key to patient survival. In an analysis of the survival of more than 400 patients with *glioblastoma multiforme* according to the old classifications, Lacroix found that only excision of more than 85% of the neuroradiologically determined tumor volume showed an improvement in patient survival compared to biopsy and limited resection, with a statistically significant difference in survival observed on resection of more than 98% of neuroradiologically established tumor volume (Lacroix et al., 2001). One of the pioneers of modern neurosurgery, Walter Dandy, reported five cases of hemispheric resection, four in patients with gliomas, despite high postoperative mortality (one patient died 48 hours after surgery due to bleeding, another after two weeks of pneumonia), the other patients

survived between three months (a patient with butterfly glioma) and three and a half years after surgery (Dandy, 1928).

Regarding tumor localization, Flores in 44 patients with *glioblastoma multiforme* according to the 2021 WHO classification and very close to our demographic characteristics found that the majority of tumors (59.1%) were located in the right cerebral hemisphere, and the most common localization is in the frontal lobe (29.5%), followed by temporal and parietal with 25% each and the rarest localization in the occipital lobe (Palpan Flores et al., 2020). Despite the differences between the two studies, Flores also concluded that the neuroradiological parameters of the tumor were comparable to those of three-dimensional reconstructions (Palpan Flores et al., 2020). In another group, similar in size and gender distribution, but with a significantly lower mean age (49.05 years), Abd-Elghany found that again the most common localization of *glioblastoma multiforme* is in the frontal lobe, followed by temporal, parietal, occipital lobe and most rarely subtentorially (Abd-Elghany et al., 2019). Despite the differences in location between the three cohorts, as in our sample, the most common location is temporal, they emphasize the heterogeneity of tumor origin from different brain structures. What unites the three cohorts is the extreme rarity of *glioblastoma multiforme* in the occipital lobes.

In a relatively large sample of gliomas, including n = 116 glioblastomas according to WHO criteria from 2016, Larjavaara found that gliomas are most often located in the frontal lobe, followed by temporal, parietal and are rare in the

occipital lobe (Larjavaara et al., 2007). In the same study of the total sample of glial tumors, it was found that the smallest tumor volume is in the occipital lobe, followed by the parietal, with the largest tumor volume in the temporal lobe with a negligible difference from the frontal (Larjavaara et al., 2007). Again, despite the difference in histogenetic criteria and the distribution of the tumor relative to the lobes, the neuroradiologically determined tumor size is entirely comparable.

6.6 Role of the systemic immune responce

The systemic immune response - studied by us on the indicators of NLR, PLR and MLR, has the potential to be a promising biomarker, given the lack of contact of the CNS with the external environment and the low incidence of inflammatory conditions of the CNS compared to other tumor sites - lung, urinary system, intestines, etc. In recent years, the scientific literature has accumulated much data on the statistical significance of preoperative NLR for patient survival (Figueroa et al., 2020; Haksoyler et al., 2021; Lei et al., 2019; Lopes et al., 2018; Weng et al., 2018). In addition, Weng found a positive correlation between the rate of increase in NLR and the histological grade of tumors of the CNS, and Haksoyler proved that the prognostic value of the index is preserved in case of recurrence of the disease (Haksoyler et al., 2021; Weng et al., 2018).

Regarding the PLR coefficient, the data are contradictory - some authors report statistical significance, while others, like us, deny it (Baran et al., 2019; Kaya et al., 2017; Kemerdere et

al., 2017; Wang et al., 2018; Yang et al., 2020). An interesting fact, supplementing the unknown significance of the PLR index, is that authors examining the combined role of NLR and PLR note that the combined coefficient has the same statistical significance as NLR itself (Kaya et al., 2017; Kemerdere et al., 2017). This correlation, which, although without statistical significance, was also established by us.

The most significant statistical significance in survival was reported in the MLR index alone and combined with other inflammatory response markers. Similar results were obtained in other studies (Baran et al., 2019; Subeikshanan et al., 2016; Zhao et al., 2020).

6.7 Physiological and some pathological aspects of Diaph3

Diaph3 is a protein belonging to the group of formins, a cytoplasmic group of proteins involved in the polymerization of actin filaments in proliferation, microtubule stabilization, cell migration, and division, and they are also an essential interface for signal transduction and the processes of intracellular regulation (Chalkia et al., 2008; Evangelista et al., 2003).

In the human body, the formin group is composed of 15 proteins divided into seven subfamilies, many of which are co-expressed in a large number of tissues (Schönichen and Geyer, 2010). The functions of Diaph3 are primarily characteristic of most of the proteins of this family, as its physiological role is to mediate the polymerization of actin molecules, stabilization of microtubules, and also has a role in

contact with the profilins - structural formation of mobile cell growths such as kinocilia and pseudopods (Palander et al., 2021). Although less studied, the protein also plays a role in cell division, participating in the stabilization of the mitotic spindle and the cytoskeleton as a whole (DIAPH3 Gene - GeneCards | DIAP3 Protein).

Functional changes in the inactivation of Diaph3 in stem cells during embryonic and fetal development are associated with mitotic errors, leading to depletion of neuronal progenitors and disturbances in the formation of epithelial cell cilia (Lau et al., 2021; Palander et al., 2021). At this stage, there is limited data on the role of the protein in diseases of the nervous system, the strongest of which exist for the autistic spectrum of diseases in loss of expression and autosomal dominant auditory neuropathy in overexpression (Vorstman et al., 2011).

Reports of the importance of Diaph3 are available in malignant tumors of the pancreas, prostate, mammary gland, liver, cervical squamous cell carcinoma, and osteosarcoma (Iwadate et al., 2010; Morley et al., 2015; Rong et al., 2021; Wan et al., 2021; Zhang et al., 2021; Expression of DIAPH3 in cancer - The Human Protein Atlas). According to the Human Protein Atlas and Foda, the prognosis with high Diaph3 expression is more favorable for colorectal carcinoma, while it is worse in lung and endometrial carcinoma (AlRahman Foda et al. 2018; Expression of DIAPH3 in cancer - The Human Protein Atlas).

From the available data on the role of Diaph3 in malignant diseases, it was found that the loss of expression leads to the so-called amoeboid phenotype - cells acquire plastic properties, which allows them to move in the extracellular matrix without destroying it (by proteolysis or induced necrosis) or to adhere to it, thus malignant cells more easily and quickly enter the lymphatic and bloodstream vessels, which favors metastatic potential (Hager et al., 2012; Wu et al., 2021). In a large group of histogenetically different tumors, the loss of Diaph3 was shown to be a time-related process - observed as a heterogeneous phenomenon with tumor advancement (Hager et al., 2012).

Although it is associated with tumor progression and favors metastatic potential, the phenomenon of Diaph3 loss may have a potentially predictive effect on the pharmacological response of tumors, given its stabilizing role in the cell's cytoskeleton. However, the role of Diaph3 in malignant tumors remains controversial and largely unclear - high expression is associated with a favorable prognosis in some and unfavorable in other groups, most likely due to multifaceted mechanisms of tumor progression - while in some tumors, it is a key participant in others, it is a side participant in tumor progression (Wan et al., 2021).

As an essential molecule whose loss allows cytoskeletal remodeling in amoeboid cell migration, Diaph3 plays a significant role in the invasion of surrounding tissues and the development of lymph node metastases in these tumors, with the most significant specificity shown in the progression of prostate, mammary and hepatocellular carcinoma where

expression in metastatic lesions is lower and weakly positive tumors have a worse prognosis (Hager et al., 2012; Kim et al., 2014; Morley et al., 2015). However, interaction has also been found in triple-negative breast carcinoma, where Diaph3 overexpression is associated with lower invasiveness and metastatic potential, hence a better prognosis (Jiang, 2017). Data also exist for squamous cell carcinoma of the cervix, where overexpression of the protein is associated with an unfavorable prognosis, while loss of expression is associated with slower progression (Wan et al., 2021). According to the authors of this report, the loss of Diaph3 correlates with the inactivation of the mTOR pathway, which is an important affector and regulator of the P13K and Akt pathways (Tian et al., 2019; Wan et al., 2021). Thus, loss of expression leads to blockade of signal transduction and cell interaction with growth factors such as EGFR and PDGF, which have a well-established role in *glioblastoma multiforme* (Akhavan et al., 2010; Nagarajan and Costello, 2009). Another interesting proven interaction of Diaph3 in this type of tumor is that loss of expression leads to increased susceptibility of these tumors to taxanes (Morley et al., 2015).

Against this background, the data on Diaph3 expression in glioblastomas shown by us is interesting. We can conclude in the first place that *glioblastoma multiforme* is a tumor with a heterogeneous expression of Diaph3. Add to this the fact that the brain tissue has little to no antibody expression, except for single positive cells in the cerebral cortex and in reactive gliosis, there is a well-presented background reaction cytoplasmic reaction for the antibody is in the growths of cells with astrocytic morphology. This makes Diaph3 a good

differential diagnostic marker in the differentiation of a tumor from reactive gliosis. Of course, this does not mean that Diaph3 is a glial-specific marker, given the expression shown in normal tissues in mobile, secreting and remodeling cells and in multiple malignancies.

If we accept these statements for intercellular interactions as valid in *glioblastoma multiforme*, then based on our results, this further emphasizes the heterogeneity of the tumor cell population. In turn, this heterogeneity is both morphological, immunophenotypic and functional. The available mechanism of avoidance of therapy is based on the functional differences in the cellular processes - the tumor stem cells that migrate through the brain parenchyma and some of the mature tumor cells with Diaph3 expression are sensitive to therapy with anti-EGFR agents and taxanes while mature tumor cells, the percentage of which is highly variable, are resistant (Wan et al., 2021). This further emphasizes the intra-tumor heterogeneity of the cell population in *glioblastoma multiforme* and the challenges in its therapy, given the differences in signaling pathways that may be affected.

Last but not least, the purely practical application of Diaph3 expression in neuropathological practice may be helpful to the neuropathologist in differentiating not only the normal parenchyma from gliosis and tumor but also in identifying tumor proliferations in neuronavigation (stereotactic) biopsies from the peripheral areas of the tumor, where the rhythmic structures of growth are well emphasized due to their strong expression of the antibody.

6.8 Predictive potential of Diaph3 as a biomarker for rapamycin and taxane treatment

One of the proposed mechanisms for the interaction of Diaph3 is in the mTOR signal transduction pathway, where the loss of expression is associated with the inactivation of this cascade (Mecca et al., 2018; Wan et al., 2021).

Results published by Wan demonstrate that high expression of Diaph3 is positively correlated with mTOR, as analysis of cell cultures showed that decreased levels of Diaph3 reduced the expression of mTOR-related proteins - p-AKT, mTOR and p-p70s6k and increased the expression of PTEN - tumor suppressor cascade (Wan et al., 2021).

Due to the potential for pharmacological effects of these mechanisms, several preclinical studies investigate the effect of rapamycin (trade name sirolimus) in treating patients with histologically verified glioblastoma (Chandrika et al., 2016; Heimberger et al., 2005; Zimmerman et al., 2020). Using cell cultures and xenographic models of glioblastoma, Arcella reported a reduction in tumor volume of up to 95% and almost twice as long survival with rapamycin therapy through induction of autophagy (Arcella et al., 2013). A clinical study on the effect of rapamycin in the treatment of patients with *glioblastoma multiforme* published by Cloughesy showed a good response in some patients, with a significant reduction in cell proliferation, no significant side effects, with adequate intratumoral drug concentration (Cloughesy et al., 2008). However, no effect was observed in almost half of the patients

and the development of resistance to therapy over time (Cloughesy et al., 2008).

Given the substantial heterogeneity of Diaph3 expression in our cohort and the mechanisms described so far, it follows that only patients with a high percentage of antibody-positive tumor cells would benefit from rapamycin. Additional evidence for this correlation is available from data on patients with tuberous sclerosis predisposed to the development of multiple tumors, including glial, in which sirolimus therapy has a preventive and antitumor effect (Li et al., 2019).

Another critical proposed role of Diaph3 in pharmacological therapy of malignancies is related to low levels of Diaph3 and sensitivity to taxanes and other drugs acting on microtubules due to cytoskeletal destabilization (Kawabata Galbraith and Kengaku, 2019; Lau et al., 2021; Morley et al., 2015). According to data published by Morley, cells with low expression of Diaph3 show increased sensitivity to taxanes, while other members of the family - Diaph1 and Diaph2 do not show such a correlation, with Diaph1 showing an inverse correlation - increased resistance with reduced expression (Morley et al., 2015).

Analysis, again by Morley, shows that several randomized clinical trials for the treatment of mammary carcinoma with taxanes report that low levels of intratumoral expression or loss of Diaph3 are associated with a better prognosis in taxane therapy (Morley et al., 2015). Similarly, data from the same report show that low levels of Diaph3 mRNA correlate with a

longer time to relapse with the same therapy (Morley et al., 2015).

Given these data and despite the substantial heterogeneity in the expression of our cohort, these mechanisms appear to be valid for *glioblastoma multiforme*, in which there are data not only on the importance of the mTOR pathway - a critical interacting unit but also on the effectiveness of taxane therapy, which increases survival in some patients (Akhavan et al., 2010; Hess et al., 2005; Iwadate et al., 2010; Sémiond et al., 2013; Stoyanov and Dzhenkov, 2017).

Against the background of conflicting data from clinical and preclinical studies on the role of taxanes and rapamycin in GBM therapy and given the similar dichotomous division in our cohort and the results reported by Arcella - a very good effect against its absence and the intracellular interactions of Diaph3, we can conclude that it is a marker with solid predictive potential in the selection of patients suitable for the abovementioned therapies.

7. Conclusions

Glioblastoma multiforme, according to WHO criteria for CNS tumors from 2021, is a malignant tumor with predominantly astrocytic differentiation, cell polymorphism, microvascular proliferation and/or pseudopalisadic necrosis and has no IDH mutation.

The tumor is extremely large, on average over 50 mm in diameter and leads to a neurological deficit, according to the affected area in the brain. Primary tumor size, location, and laterality of the process did not affect patient prognosis. Statistical significance concerning the age of diagnosis was found only between the age groups 41-50 years and over 70 years.

The main factor determining the prognosis of patients is the mutational status of MGMT, which shows the possibility of conventional treatment of the tumor through temozolomide therapy, where the difference in survival between the two groups is extremely large, not only when comparing the average survival but also the survival on the first, the second and third year.

Despite the relative autonomy of the nervous system concerning the immune response, the statistical significance in the survival of patients with an acute-phase response and/or reduced stress immunity is high. According to the obtained results, the ratio of monocytes to lymphocytes from preoperative blood counts is of tremendous statistical significance, and the increase of this coefficient is a poor prognostic sign.

Glioblastoma multiforme is a Diaph3 positive tumor, with positivity being heterogeneous - strong in areas of tumor growth where tumor stem cells are present, while a large proportion of mature tumor cells are tumor negative. No correlation of expression levels with patient prognosis and tumor size was found but given the established interactions of the protein with signal transduction pathways, Diaph3 is a candidate biomarker showing tumor sensitivity to taxanes.

8. Contributions

8.1 Diagnsotic and clincal contributions

- the correlation between the neuroradiological parameters in *glioblastoma multiforme* and the volume analyses of three-dimensional reconstructions performed by them was confirmed

- the predilection sites for the development of *glioblastoma multiforme* - frontal, temporal and parietal lobe, without any difference in gender, age and laterality of the process have been identified

- the average neuroradiological size of *glioblastoma multiforme* was established - a little over 50 mm at the time of diagnosis, varying in the range of 20-76 mm

- the importance of the expression of the anti-Diaph3 antibody in the diagnosis of tumors of the nervous system has been established

- the form of expression of the anti-Diaph3 antibody in the normal brain parenchyma, in reactive gliosis and *glioblastoma multiforme* has been established

- no correlation was found between Diaph3 expression levels and survival and primary tumor size

8.2 Therapeutic contributions

- the role of the systemic immune response in the prognosis of patients with *glioblastoma multiforme* has been established

- the critical importance of MGMT mutation status in patients with *glioblastoma multiforme* has been confirmed

- the importance of Diaph3 expression as a possible predictive factor for the treatment of GBM with taxanes and rapamycin is argued.

9. Publications of the topic

9.1 Conference proceedings

G. Stoyanov, E. Lutfi, D., Dzhenkov, L. Petkova. The role of Diaph3 in the growth of *glioblastoma multiforme*. JUBILEE SCIENTIFIC CONFERENCE - 60 YEARS OF PATHOPHYSIOLOGY - MEDICAL UNIVERSITY - VARNA. September 24 - 25, 2021, Varna, Bulgaria.

9.2 Journal publications

9.2.1 In international journals

9.2.1.1 In indexed journals with an impact factor

Stoyanov G, Kitanova M, Dzhenkov D, Ghenev P (2019) The diagnostic dilemma of epithelial marker expression in glioblastoma. Pathology & Oncology Research, 25(2), 809-810.

Stoyanov GS, Dzhenkov D, Ghenev P, Iliev B, Enchev Y, Tonchev AB (2018) Cell biology of *glioblastoma multiforme*: from basic science to diagnosis and treatment. Medical Oncology, 35(3), 1-10.

9.2.1.2 In indexed journals withput an impact factor

Stoyanov GS, Petkova L, Dzhenkov DL (2019) Hans Joachim Scherer and his impact on the diagnostic, clinical, and modern research aspects of glial tumors. Cureus, 11(11).

Stoyanov GS, Petkova L, Dzhenkov DL (2019) A Practical Approach to the Differential Diagnosis of Intracranial Tumors: Gross, Histology, and Immunoprofile-based Algorithm. Cureus, 11(12).

Stoyanov GS, Sarraf JS, Matev BK *et al.* (2018) A comparative review of demographics, incidence, and epidemiology of histologically confirmed intracranial tumors in Brazil and Bulgaria. Cureus, 10(2).

Stoyanov GS, Dzhenkov DL (2018) On the Concepts and History of *Glioblastoma multiforme*-Morphology, Genetics and Epigenetics. Folia medica, 60(1), 48-66.

Stoyanov GS, Dzhenkov DL, Kitanova M, Donev IS, Ghenev P (2017) Correlation between Ki-67 Index, world health organization grade and patient survival in glial tumors with astrocytic differentiation. Cureus, 9(6).

Stoyanov GS, Dzhenkov DL, Kitanova M, Ghenev P, Tonchev AB (2017) Demographics and incidence of histologically confirmed intracranial tumors: a five-year, two-center prospective study. Cureus, 9(7).

9.2.1.3 In international, non-indexed journals

Lyutfi EM, Georgieva R, **Stoyanov GS**, Dzhenkov D. (2020). Tumor growth patterns in central nervous system tumors with astrocytic differentiation. Glioma, 3(2), 67.

Georgieva R, Lyutfi E, **Stoyanov GS**, Dzhenkov D. (2020). CD34 neural progenitor cells in *glioblastoma multiforme*. Glioma, 3(1), 13.

Stoyanov GS (2019) The 2016 revision of the World Health Organization classification of tumors of the central nervous system: Evidence-based and morphologically flawed. Glioma, 2(4), 165.

9.2.2 In national journals

Stoyanov GS, Dzhenkov D, Ghenev P (2017) Cytokeratin AE1/AE3 mimicry in glioblastoma. Scripta Scientifica Medica, 49(1), 47-52.

Stoyanov GS, Dzhenkov D, Ghenev P. (2017). The Great Imitator-EMA positive *glioblastoma multiforme*. Scripta Scientifica Medica, 49(1), 21-25.

10. Thank you

I want to thank my research supervisor - Prof. Petar Genev, MD, PhD, for the opportunity to be his doctoral student and the constructive criticism he directed towards the work done and the design of the dissertation.

Thanks to my scientific consultant - Assoc. Prof. Stoyan Pavlov, MD, PhD for the methodological guidelines in the work process.

Thanks to my teacher - Assoc. Prof. Deyan Dzhenkov, MD, PhD, for introducing me to neuropathology and for all the help in selecting materials.

I thank my mentors - Prof. Anton Tonchev, MD, PhD, DSc, Assoc. Prof. Nikolay Sapundjiev, MD, PhD and Assoc. Prof. Kamelia Bratoeva, MD, PhD for all the efforts and opportunities given to me to develop.

I want to thank Petar Valchanov, MD, from the Department of Anatomy and Cell Biology for the methodological support in carrying out the three-dimensional reconstructions.

I thank the laboratory assistant Svetla Kostadinova for the precision with which she prepared the slides for the dissertation and the late Elena Boeva for introducing me to the subtleties of this art.

Thanks to Lilyana Petkova, MD, for the continuous support in the work process.

I thank Hristo Popov, MD, PhD, Ina Kobavoka, MD, PhD, laboratory assistant Iveta Dangova and hall attendant Violeta Zhelyazkova for the daily support and courage they inspired me with.

I want to thank my colleagues from the Department of General and Clinical Pathology, Forensic Medicine and Deontology, headed by Prof. Maria Tsaneva, MD, PhD, for their help in difficult times.

Thanks to my colleagues and friends - Emran Lutfi, MD and the future MD - Reneta Georgieva for the methodological support and inexhaustible energy and enthusiasm for work.

Thanks to my colleagues from the Department of Anatomy and Cell Biology, the Department of Physiology and Pathophysiology, the Department of Imaging, Interventional Radiology and Radiotherapy and the Department of Neurology and Neuroscience for their help in collecting cases and interpreting the results.

Last but not least, I thank my family for the fact that they paid the price for me to get here with their work and faith in me.

THANK YOU!